

# Tacticity Influence on the Electrochemical Reactivity of Group Transfer Polymerization-Synthesized PTMA

Hugo A. López-Peña,<sup>†</sup> Lindsay S. Hernández-Muñoz,<sup>‡</sup> Bernardo A. Frontana-Uribe,<sup>§,⊥</sup> Felipe J. González,<sup>‡</sup> Ignacio González,<sup>†</sup> Carlos Frontana,<sup>\*,‡,||</sup> and Judith Cardoso<sup>\*,†</sup>

<sup>†</sup>Universidad Autónoma Metropolitana-Iztapalapa Av., San Rafael Atlixco 186, Col. Vicentina 09340, México, DF, Mexico

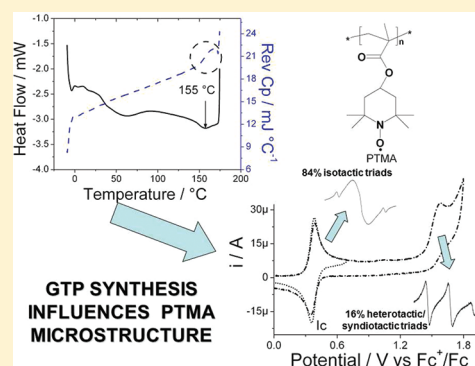
<sup>‡</sup>Centro de Investigación y Estudios Avanzados, Departamento de Química, Av. Instituto Politécnico Nacional No. 2508, Col. San Pedro Zacatenco, C. P. 07360. México, DF, Mexico

<sup>§</sup>Centro Conjunto de Investigación en Química Sustentable, UNAM-UAEM, Km. 14.5 Carretera Toluca-Atlaconulco, C. P. 50200, Toluca, Estado de México, DF, Mexico

<sup>⊥</sup>Academic of the Instituto de Química, UNAM, México, DF, Mexico

## Supporting Information

**ABSTRACT:** Spectroscopic, thermal, and electrochemical characterization results are presented for the redox active polymer poly(2,2,6,6-tetramethyl-1-piperinidyl-4-yl methacrylate) or PTMA, synthesized by group transfer polymerization (GTP), and its precursors 4-hydroxy-tetramethylpiperidine-*N*-oxyl (HO-TEMPO) and 4-methacryloyloxy-tetramethylpiperidine-*N*-oxyl (MO-TEMPO). DSC analysis of synthesized PTMA showed that the glass transition temperature ( $T_g$ ) of the polymer structure occurs at 155 °C, corroborated by dynamic mechanical analysis (DMA), which is higher when compared with  $T_g$  data for PTMA synthesized by other methods. Also, the amount of radical species present in PTMA synthesized by GTP reactions (100%) is higher than the values typically upon synthesizing PTMA by radical polymerization. Electrochemical and spectroelectrochemical-electron spin resonance studies in acetonitrile revealed two redox events in the PTMA polymer, one of which is reversible, accounting for ca. 80% of the spins in the polymer and giving rise to the battery behavior. The other redox event is irreversible, accounting for the remaining ca. 20% of spins, which has not previously been reported. These two redox events are linked to a structural property associated with the tacticity of the polymer, where the reversible feature (responsible for cathode behavior) is the dominant species. This corresponds to a number of isotactic domains of the polymer (determined by high temperature <sup>1</sup>H NMR). The second feature accounts for the three-line impurity observed in the ESR, which has been reported previously but poorly explained, associated to the number of heterotactic/syndiotactic triads.



## INTRODUCTION

Design and construction of lithium-ion batteries, working as operative rechargeable batteries is an active field of study,<sup>1,2</sup> due to their use as power sources for high performance electronic devices. Development of materials providing the basis for performance-improvement is therefore a key issue during active research, and in this context, several materials have been tested;<sup>3,4</sup> this is a critical point when considering the underlying conflict between power capability and energy density output in the battery.<sup>5</sup>

Polymers bearing TEMPO or *N*-oxy radical species act as alternative materials, due to the reversible properties of their electrochemical conversion, rendering them usable as anode materials in operating battery systems.<sup>6–9</sup> Poly(2,2,6,6-tetramethyl-1-piperinidyl-4-yl methacrylate) or PTMA (3) is particularly useful as a cathode material for lithium-ion rechargeable batteries,<sup>9–12</sup> in which high charge/discharge efficiencies have been achieved.<sup>5</sup> This polymer is built from repeated nitroxide radical moieties, which present reversible oxidation processes forming stable oxoammonium cations.

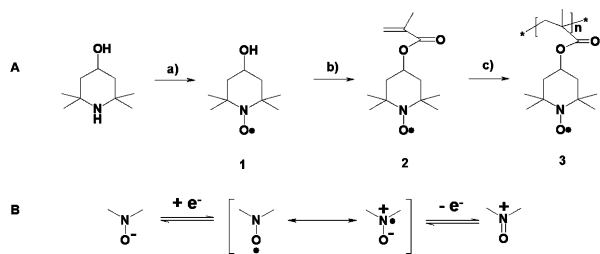
Synthetic procedures previously described for PTMA (3) generate nitroxide radicals at the last stage of the process by oxidizing the polymer obtained, from either 4-methacryloyloxy-2,2,6,6-tetramethylpiperidine or 4-methacryloyloxy-*N*-hydroxy-2,2,6,6-tetramethylpiperidine, via a free radical polymerization reaction.<sup>13</sup> Unfortunately, this oxidation reaction does not proceed with a 100% oxidation yield and affords PTMA containing only 65% to 81% of the theoretically possible amount of redox active nitroxide groups. An alternative synthetic method for PTMA from compound 2 (Scheme 1A) is to employ group transfer polymerization (GTP) reactions;<sup>14</sup> this method has the advantage of yielding a higher number of repetitive units containing the redox radical species per mass unit of the polymer, leading to an increase of charge capacity of the corresponding device.<sup>14</sup>

Received: February 7, 2012

Revised: April 13, 2012

Published: April 17, 2012

**Scheme 1.** (A) Synthesis of Poly(4-methacryloyloxy-2,2,6,6-tetramethylpiperidine-*N*-oxyl) (PTMA, 3): (a)  $\text{HPWO}_4$ ,  $\text{H}_2\text{O}_2$ , (b) Methacryloyl Chloride,  $\text{NEt}_3$ ,  $\text{PhCH}_3$ , (c) 1-Methoxy-2-methyl-1-trimethylsilyloxy-propene, TBAF, THF; (B) Reduction and Oxidation Processes for Nitroxide Radicals



Interestingly, only scarce attention has been devoted to the microstructure present in the final synthesized PTMA structure,<sup>7–12</sup> which could be related to the change in charge capacity of the polymer structure, due to the different types of arrangements that the radical species would present as a result of the polymerization process. These effects can also influence the energy required to oxidize these radical structures, which must be related to the high charge/discharge potentials attainable during normal operation of batteries. For this purpose, in this work, PTMA (3) and two precursor molecules 1 and 2 were extensively characterized using NMR, in particular polymer tacticity, and mass spectrometry; also the stability of PTMA was evaluated using thermal analysis, and finally, electrochemical and spectroelectrochemical-electron spin resonance studies in acetonitrile solution provide a systematic evaluation of the structural factors determining the reactivity in the final polymeric structure.

## EXPERIMENTAL SECTION

**Synthesis of Poly(4-methacryloyloxy-2,2,6,6-tetramethylpiperidine-*N*-oxyl) (PTMA, 3).** 4-Hydroxy-2,2,6,6-tetramethylpiperidine-*N*-oxyl (HO-TEMPO, 1) was obtained from 4-hydroxy-2,2,6,6-tetramethylpiperidine oxidation according to the procedure described by Brière,<sup>15</sup> employing a reaction time of 8 h (Scheme 1A). The final compound was recrystallized from hexane: mp 72 °C (Lit. 72 °C).<sup>15</sup> 4-Methacryloyloxy-2,2,6,6-tetramethyl piperidin-*N*-oxyl (MO-TEMPO, 2) was obtained from compound 1 and methacryloyl chloride following the procedure described by Nesvadba and co-workers.<sup>14</sup> The obtained compound was recrystallized from hexane, mp 88–89 °C (mp 91–92 °C).<sup>16</sup> PTMA (3) was synthesized according to the GTP reaction described earlier,<sup>14</sup> using 1-methoxy-2-methyl-1-trimethylsilyloxy-propene as initiator and tetrabutylammonium fluoride (TBAF) as catalyst in tetrahydrofuran (THF). The reaction was stirred for 48 h with 3 additions of the catalyst (1:1250 with respect to the amount of monomer used) during this period.

**Characterization of PTMA.** Chemical structures for molecules 1, 2, and 3 were analyzed by <sup>1</sup>H and <sup>13</sup>C NMR ( $\delta$  = ppm,  $J$  = Hz), (Bruker DMX 500 MHz) in 5–10% weight solution of  $\text{CDCl}_3$  with tetramethylsilane (TMS) as an internal reference.

PTMA tacticity was determined by employing <sup>1</sup>H NMR ( $\delta$  = ppm,  $J$  = Hz), (Varian MR 400 MHz) at 160 °C in a 16.7 mg mL<sup>-1</sup> solution in a mixture of solvents (41.7% *o*-dichlorobenzene, and 58.3% deuterated DMSO, which was used as reference).  $\text{PhNHNH}_2$  (10.1 × 10<sup>-3</sup> mg mL<sup>-1</sup>) was used

for quenching the nitroxide moiety. The deconvolution procedure is presented in the Supporting Information.

Mass spectra were recorded on a JEOL JMS-AX 500SHA spectrometer using electron impact (EI). Elemental analysis (Elemental Perkin-Elmer 2400 CHNS/O Series II) was used to verify the chemical composition of the polymer. Molecular weight was determined at room temperature using a gel permeation chromatography (GPC) apparatus with a light scattering detector Dawn-EOS (Wyatt Tech.) at  $\lambda$  = 6900 Å in THF with a flow rate of 0.5 mL min<sup>-1</sup>. Refractive index increment  $dn/dc$  for the polymer was calculated as 0.109 mL g<sup>-1</sup> in both the same solvent and wavelength using a Brice-Phoenix Visual Refractometer. Thermal behavior was determined using a MDSC2920 Modulated Differential Scanning Calorimeter manufactured by TA Instruments (Newcastle, Delaware, USA). Modulated DSC scans were carried out at 5 °C/min with amplitude of  $\pm 0.5$  °C, a period of 40 s, and a 50 mL min<sup>-1</sup> nitrogen flow within the range of -50 to 180 °C. A similar analysis was performed using a Thermogravimetric Analyzer Pyris 1 TGA, Perkin-Elmer, at a heating rate of 10 °C min<sup>-1</sup> under a 50 mL min<sup>-1</sup> nitrogen flow within the range of 45 to 700 °C. Dynamic mechanical analysis (DMA) was performed using a stress-controlled CVO rheometer (Malvern Instruments). A temperature scan was performed in shearing mode at 1 Hz ranging from 120 to 210 °C; using a heating rate of 2 °C min<sup>-1</sup>. Measurements of the magnetic susceptibility of PTMA were performed with direct current SQUID equipment (IIM-UNAM).

**Voltammetric and Electrochemical-Electron Spin Resonance Measurements.** Acetonitrile ( $\text{CH}_3\text{CN}$ ) Merck Spectroscopic grade, distilled from  $\text{P}_2\text{O}_5$  and kept under molecular sieves (3 Å, Merck), was used as solvent. Recrystallized tetrabutylammonium hexafluorophosphate from methanol/ethyl acetate (Fluka Chemika, electrochemical grade,  $\text{NBu}_4\text{PF}_6$ ) was used as the supporting electrolyte. All the solutions were purged with high purity argon (Praxair, grade 5.0) for 25 min before each series of experiments. Cyclic voltammetry experiments were performed with an AUTOLAB PGSTAT 100 potentiostat/galvanostat. IR Drop correction was performed during all of the experiments.<sup>17,18</sup> A three electrode cell was used to carry out these experiments: a glassy carbon microelectrode (surface, 0.07 cm<sup>2</sup>) was used as the working electrode. Prior to use, it was polished with 0.05  $\mu\text{m}$  alumina powder (Bühler), sonicated in distilled water for 10 min, and rinsed with acetone; rinsing with acetone was also performed between each voltammetric run. A platinum mesh was used as an auxiliary electrode. Potential values were obtained versus a commercial Saturated Calomel Electrode (SCE) separated from the solution by a salt bridge and referenced to the ferricinium/ferrocene couple ( $\text{Fc}^+/\text{Fc}$ ) according to the IUPAC recommendation.<sup>19</sup> The potential value of this redox couple versus the reference electrode was  $0.40 \pm 0.01$  V.

ESR spectra were recorded in the X band (9.85 GHz), using a Bruker EMX Plus instrument with a rectangular TE<sub>102</sub> cavity. A commercially available spectroelectrochemical cell (Wilmad) was used. A platinum mesh (0.7 cm<sup>2</sup>) was introduced into the flat path of the cell and used as a working electrode. A platinum wire was used as an auxiliary electrode (2.5 cm<sup>2</sup>).  $\text{Ag}/\text{AgNO}_3$  0.01 mol L<sup>-1</sup> + 0.1 mol L<sup>-1</sup>  $\text{NBu}_4\text{PF}_6$  in acetonitrile was employed as the reference electrode. Potential control was performed with an AUTOLAB PGSTAT 100 potentiostat.

## RESULTS AND DISCUSSION

**Synthesis and Characterization of PTMA.** Synthesis of PTMA was carried out by employing a group transfer polymerization (GTP) reaction (Scheme 1) according to Bugnon et al.<sup>14</sup> A complete description of <sup>1</sup>H and <sup>13</sup>C NMR spectra for compounds 1, 2, and 3 is presented in the Supporting Information for this article. Elemental analysis for the synthesized PTMA structure, C (64.97%); H (9.23%); N (5.83), corrected due to water presence in the sample (see below), is in agreement with percentages calculated for C<sub>13</sub>H<sub>22</sub>NO<sub>3</sub> (240.33): C (62.88%); H (9.22); N (5.64%), confirming also the structure proposed. The obtained polymer presented a molecular weight of 36 240 g mol<sup>-1</sup> with a polydispersity  $M_w/M_n$  of 1.532 ( $M_w$  and  $M_n$  represent the molecular weight and number averaged molecular weight, respectively), indicating a mean content of 151 repetitive units. PTMA was soluble in tetrahydrofuran, chloroform, and acetonitrile.

Thermal stability of 3 obtained by GTP was studied by employing a combined analysis using TGA and derivative thermogravimetric analysis (DTGA). Synthesized PTMA was stable up to 200 °C (Figure 1), and the decomposition temperature

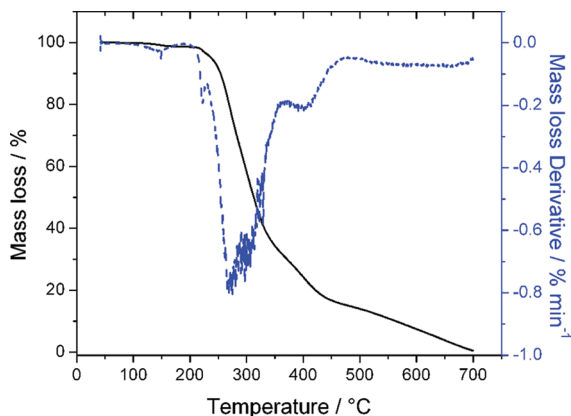


**Figure 1.** Thermogravimetric and differential thermogravimetric analysis plots for PTMA.

(corresponding to 10% of weight loss) was observed at 270 °C, close to a previously reported value (263 °C).<sup>20</sup> A weight loss of 3% that approximately ends at 170 °C (Figure 1) was associated with water elimination of the sample. Thermal degradation of PTMA showed two degradation steps starting around 200 and 400 °C. However, a closer inspection of DTGA curves of PTMA showed that the first degradation step is composed of two overlapped peaks, one sharp signal at 275 °C and another wide and ill-defined signal around 300 °C. The first decomposition step, which includes the two overlapping peaks mentioned, corresponds to 67% of weight loss and is associated with 161.02 g mol<sup>-1</sup> of the total molar mass of each repetitive unit, corresponding to the elimination of a piperidine ring derivative (154 g). The second step (16% of weight loss, corresponding to 38 g mol<sup>-1</sup> considering the molar mass of each repetitive unit) is associated to decarboxylation of the resulting polymer after the first decomposition in accordance with previous reports.<sup>21</sup>

Differential scanning calorimetry (DSC) and thermogravimetric analysis (TGA) were used to determine the glass transition temperature ( $T_g$ ) and thermal stability of the polymer, respectively. The glass transition temperature  $T_g$  for PTMA was

determined by modulated differential scanning calorimetry (MDSC) and confirmed by dynamic mechanical analysis (DMA, see below). MDSC trace for reversible heat obtained from the second heating is shown in Figure 2, from which the

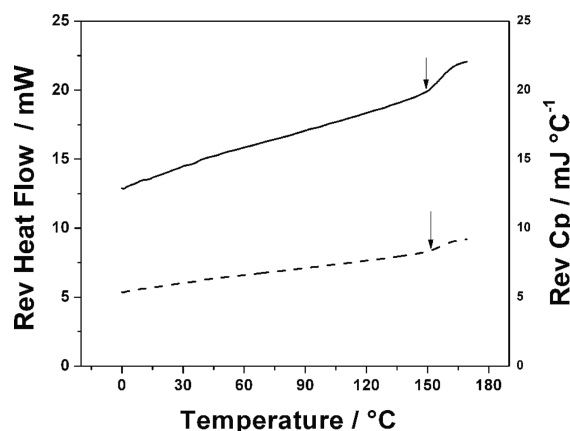


**Figure 2.** Variations of reversible heat flow (solid line) and reversible  $C_p$  (dashed line) employing MDSC analysis (third scan plotted). Arrows indicate the beginning of  $T_g$ .

$T_g$  value occurred at 153 °C. This value is significantly higher than the previously reported value of 76 °C for PTMA synthesized by radical polymerization.<sup>22</sup> As the  $T_g$  is a quasi-reversible property, its value could also be confirmed by evaluating the reversible  $C_p$  curve in the thermogram obtained by modulated DSC. This shows a variation in the reversible  $C_p$  starting at 153 °C. Also, no changes in the reversible  $C_p$  value were observed at the temperature range around the  $T_g$  value (76 °C) reported by Kim and co-workers,<sup>23</sup> thus confirming that PTMA obtained by GTP shows different properties to that obtained by radical polymerization. The glass transition temperatures were further verified by carrying out dynamic mechanical analysis (DMA). The storage shear modulus ( $G'$ ) and the viscous shear modulus ( $G''$ ) as a function of temperature for PTMA are shown in Figure 3. In dynamic mechanical

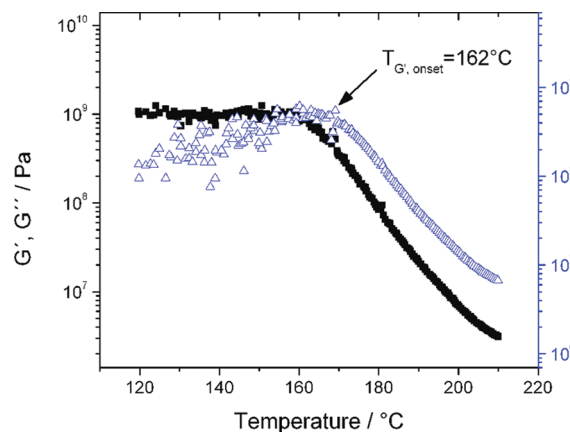


**Figure 3.** Storage (■) and loss shear (Δ) moduli at 1 rad s<sup>-1</sup> plotted against temperature for PTMA. Onset occurs at 162 °C.

analysis, the glass transition temperature can be measured, while the temperature is scanned, although it is not uniquely defined because it is dependent on the frequency applied, and it is also conventionally determined by either the onset in the

storage modulus  $G'$  ( $T_{g,G'}$ ) or the temperature at maximum in the loss modulus  $G''$  ( $T_{g,G''}$ ). The peak at 167 °C is attributed to the  $\alpha$  mechanism associated with the transition from glasslike to rubberlike consistence.<sup>24,25</sup> The value of 162 °C obtained in onset of  $G'$  is close to the  $T_g$  value obtained by DSC (Figure 2). This small difference in  $T_g$  values is usually obtained upon comparing results from DMA and DSC techniques.<sup>26</sup>

The high  $T_g$  value found in this work for PTMA could be associated to the ability of the nitroxide (NO) groups to act as acceptors of hydrogen bonds and the possibility of the formation of hydrogen-bonded networks.<sup>20,27–30</sup> SQUID measurements revealed that the magnetic susceptibility of PTMA differs from the expected behavior for a paramagnetic material at low temperatures (Figure 4), revealing a certain ferromagnetic

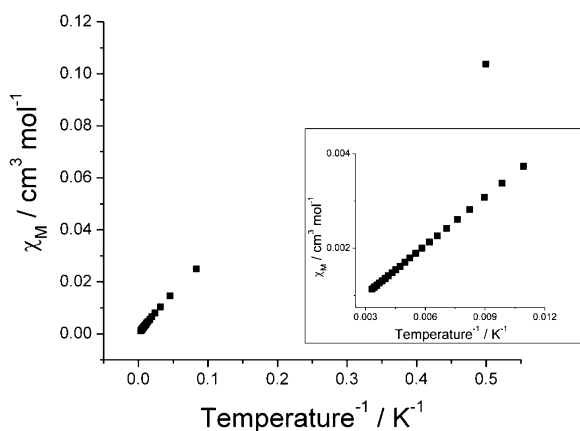


**Figure 4.** Variations of molar magnetic susceptibility ( $\chi_M$ ) as a function of temperature. Inset represents the variations for  $T > 81$  K.

nature of this polymer<sup>31</sup> and supporting the proposal referred above. Regardless of the nature and strength of these interactions, aggregates must be favored by increased radical concentration because PTMA has a radical per repetitive unit, so that above a certain concentration level, several kinds of aggregates may coexist.<sup>32</sup> These aggregates and interactions diminish the flexibility of the chain of polymer and then  $T_g$  must increase.

**Spectroscopic Characterization of PTMA and Its Precursors.** The precursors of PTMA were characterized by NMR and mass spectrometry corroborating the proposed structures (1 and 2 in Scheme 1) (Supporting Information shows the spectroscopic characterization of the PTMA precursors). PTMA (3) obtained by GTP reactions<sup>33</sup> was characterized by  $^1\text{H}$  and  $^{13}\text{C}$  NMR. Because of the paramagnetic effect of the N–O radical, the spectrum showed poor resolution, lacking also of signals corresponding to the TEMPO unit ( $^1\text{H}$  and  $^{13}\text{C}$  NMR, Figure SI-11A and Figure SI-11B, Supporting Information respectively). Therefore, treatment of the polymer with phenylhydrazine allowed obtaining the spectra of the corresponding hydroxylamine of 3 with the complete number of NMR signals of hydrogen and carbon atoms in PTMA. Figure 5 shows the  $^1\text{H}$  NMR spectrum of PTMA after reduction with an excess of phenylhydrazine. Polymer formation was deduced as only aliphatic protons are exclusively observed.

$^{13}\text{C}$  NMR spectrum (Figure 6, signal assignment is shown in the spectra) showed the presence of the ester function at  $\delta = 175.6$  and the presence of two methylene groups as a broad

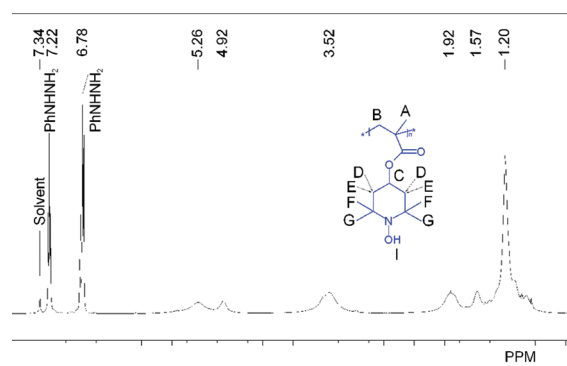


**Figure 5.**  $^1\text{H}$  NMR of poly(4-methacryloyloxy-TEMPO) (PTMA, 3) 5–10% weight in solution of  $\text{CDCl}_3$  and chemically reduced with an added excess of phenylhydrazine. The spectrum was obtained at room temperature.

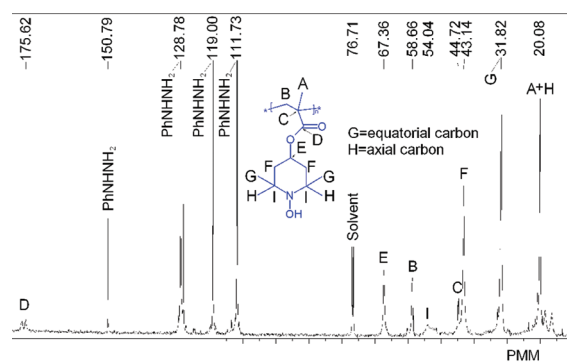


**Figure 6.**  $^{13}\text{C}$  NMR of poly(4-methacryloyloxy-TEMPO) (PTMA, 3) 5–10% weight in solution of  $\text{CDCl}_3$  and chemically reduced with an added excess of phenylhydrazine. The spectrum was obtained at room temperature.

signal at 43.1, and a quaternary carbon appeared at 44.7 ppm. Both gem dimethyl carbons are fused in a large singlet (31.8 ppm) and the methyl group of the backbone chain was assigned to the signal at  $\delta = 20.08$ . DEPT experiment of the reduced PTMA (Figure SI-12, Supporting Information) confirmed that the signal at  $\delta = 67.3$  ppm corresponds to the oxygen base methyne, and the methylene in the chain is located at  $\delta = 58.6$  ppm. All these signals confirm the PTMA structure.

Bovey and co-workers<sup>32,33</sup> have found that the signals of interest for the  $^1\text{H}$  NMR microstructural elucidation of methacrylic polymers are those corresponding to  $\alpha$ -methyl and  $\beta$ -methylene. In the case of PTMA, we have found some difficulties in the experimental NMR determination of tacticity due to the fact that signals corresponding to axial and equatorial protons, at positions 3 and 5 of piperidine ring, overlap with signals of methylene groups in the polymer backbone. Similarly, signals of methyl groups at positions 2 and 6 of piperidine ring overlap with those of  $\alpha$ -methyl. Polymers confer a high viscosity to their solutions through entanglement and through entrapment of solvent molecules. If molecular motion is allowed to take place, i.e., by raising the temperature, a narrowing of the resonance line will be observed due to the relaxation time increased,<sup>33</sup> and therefore, deconvolution is easier. In order to solve such overlapping and quantify the areas of the relevant signals  $^1\text{H}$  NMR spectra were obtained at 160 °C in a solvent mixture of o-DCB and  $d_6$ -DMSO; a deconvolution of the NMR signals at these spectra was carried out, and experimental NMR determination of tacticity was achieved.

After deconvolution (see Supporting Information for the deconvolution strategy), signals were assigned as shown in Figures 7 and 8.

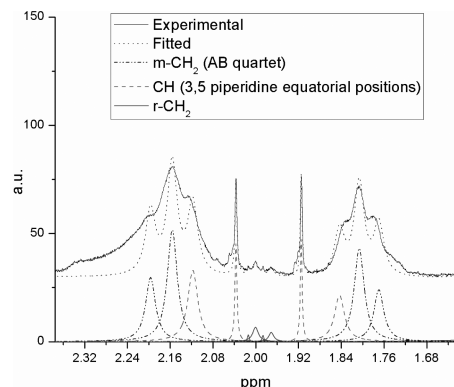


**Figure 7.** Methylenic portion of the  $^1\text{H}$  NMR spectrum for PTMA, **3** chemically reduced with phenylhydrazine in *o*-dichlorobenzene and deuterated DMSO solution. Assignments are shown in the spectrum. The spectrum was obtained at 160  $^\circ\text{C}$ .

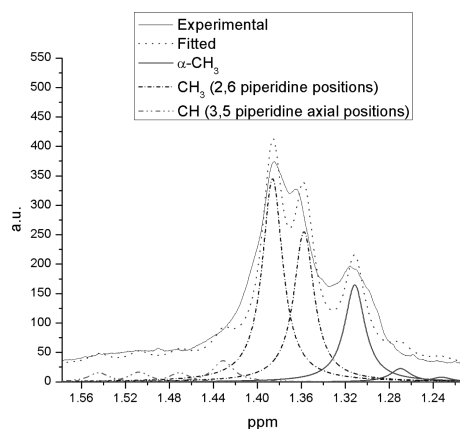


**Figure 8.** High-field portion of the  $^1\text{H}$  NMR spectrum for PTMA (**3**) chemically reduced with phenylhydrazine in *o*-dichlorobenzene and deuterated DMSO solution. Assignments are shown in the spectrum. The spectrum was obtained at 160  $^\circ\text{C}$ .

In fact, signals labeled as an AB quartet in Figure 7 are centered at 1.98 ppm, and the AB quartet has a coupling constant of 15.46 Hz. Both facts strongly correlate with evidence found by Bovey et al. for PMMA of an AB quartet centered at 2.09 ppm and a coupling constant of 14.9 Hz.<sup>32–34</sup> This AB quartet is associated with an isotactic microstructure, and the signals at the center of the quartet are related with a syndiotactic one.<sup>31–33</sup> The former is related to meso dyads and the latter with racemo ones.<sup>31,32</sup>

Figure 8 shows three signals at 1.31, 1.27, and 1.23 ppm. The chemical shifts of these signals strongly resemble the values of 1.33, 1.21, and 1.1 ppm found for PMMA by Bovey et al. for iso-, hetero-, and syndiotactic triads, respectively.<sup>32,33</sup> Integration of the areas of the  $\alpha$ -methyl peaks allowed the quantification of their normalized frequencies as 0.84, 0.12, and 0.04 for (mm), (mr), and (rr), respectively. Use of these values and well-known mathematical relationships between dyads and triads yield frequencies of 0.9 and 0.1 for (m) and (r) dyads, respectively.<sup>33,35</sup> Experimental determination of (m) and (r) produces values of 0.95 and 0.05, respectively. Considering the

great overlapping of signals, the match between calculated and experimental quantities could be considered as satisfactory and proves that signal assignment after deconvolution is reasonable. The facts described above validate the assertion that PTMA synthesized by GTP, at the experimental conditions used in this work, is a polymer with 84% of isotactic triads, 12% of heterotactic triads, and 4% of syndiotactic triads (the combined percentages of hetero- and syndiotactic triads is 16% of the total triads).

**Electrochemical and Spectroelectrochemical-ESR Study of the Nitroxide Containing Monomers and PTMA.** In order to understand the effect that structural modifications have on the stability of the nitroxide radical, an electrochemical and spectroelectrochemical-electron spin resonance (ESR) study of compounds **1** and **2** and the polymer **3** was performed. For compound **1**, the corresponding cyclic voltammogram (Figure 9A) shows the reversible mono-electronic process (peaks

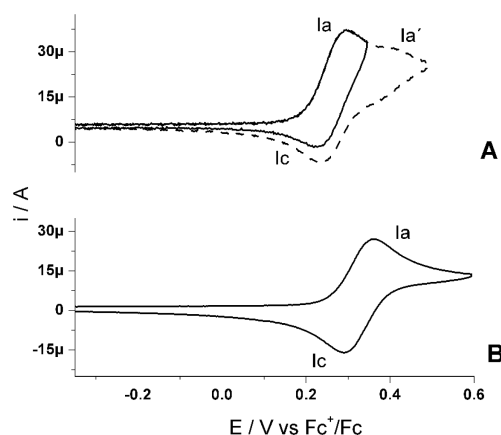


**Figure 9.** Cyclic voltammograms for (A)  $1 \times 10^{-3} \text{ mol L}^{-1}$  **1** and (B)  $1 \times 10^{-3} \text{ mol L}^{-1}$  **2** in  $0.1 \text{ mol L}^{-1} \text{ Bu}_4\text{NPF}_6/\text{CH}_3\text{CN}$ . WE, GC (0.07  $\text{cm}^2$ );  $\nu = 100 \text{ mV s}^{-1}$ . All voltammetric signals are indicated.

Ic and Ia,  $E^0 = 0.26 \text{ V vs Fc}^+/\text{Fc}$ ,  $\Delta E_p = 62 \text{ mV}$ ). A shoulder signal was observed after this oxidation process (peak Ia'), which did not affect the reversible behavior of the system Ia/Ic. This signal is probably related to an impurity present in the original commercial sample.

In the case of **2**, a reversible one-electron transfer (peaks Ia and Ic;  $E^0 = 0.32 \text{ V vs Fc}^+/\text{Fc}$ ,  $\Delta E_p = 71 \text{ mV}$ , Figure 9B), in a similar fashion as occurred for compound **1** (Figure 9A) was observed. This oxidation process is the only one appearing in the electrochemical window of the employed medium. The difference in  $E^0$  values for both compounds is associated to the inductive effect of the methacryloyloxy group at position C-4, acting as an electron-withdrawing group, leading compound **2** to become less prone to oxidation, increasing its  $E^0$  value compared to that of compound **1**.<sup>36,37</sup> This effect is relevant, as the molecule lacks  $\pi$  conjugation to consider this effect as resonant, and would therefore be regarded as a field-inductive effect.<sup>37</sup>

Compounds **1** and **2** presented paramagnetic activity, characterized by the presence of an organic radical signal with hyperfine couplings related with the interaction between the electronic spin of the unpaired electron and the nuclear spin of the adjacent nitrogen atom (Figure 10; **1**, HFCC = 15.66 G; **2**, HFCC = 15.55 G) generating a triplet structure. These signals disappear progressively with time by setting the applied potential in a spectroelectrochemical cell at 0.34 and 0.44 V vs  $\text{Fc}^+/\text{Fc}$ , respectively (Figure 10A,B). This result

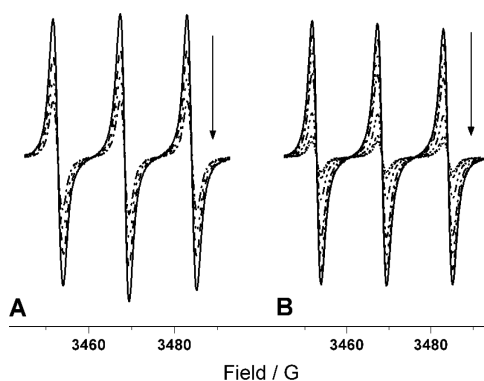


**Figure 10.** Spectroelectrochemical-ESR spectra of (A)  $1 \times 10^{-3}$  mol  $L^{-1}$  **1** and (B)  $1 \times 10^{-3}$  mol  $L^{-1}$  **2** in  $0.1$  mol  $L^{-1}$   $Bu_4NPF_6/CH_3CN$ . WE, Pt ( $0.7$  cm $^2$ ); applied potential, A,  $0.34$  V vs  $Fc^+/Fc$  and B,  $0.44$  V vs  $Fc^+/Fc$ . Arrows indicate increasing electrolysis times that provoke signal disappearance.

indicates that the observed voltammetric peaks correspond to the monoelectronic oxidation of the nitroxide radical generating the corresponding oxoammonium cation (Scheme 1B).

PTMA shows a different electrochemical and spectral behavior.<sup>38</sup> Cyclic voltammograms for PTMA show the presence of signal Ia/Ic (Figure 11); as a reversible electron

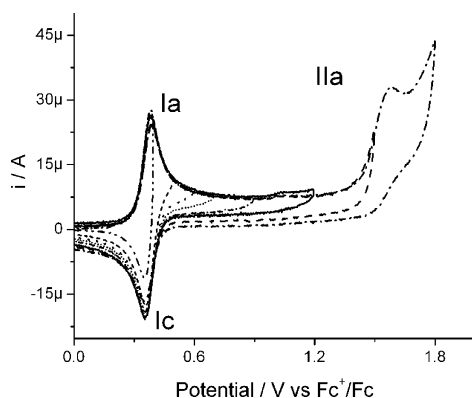


**Figure 11.** Cyclic voltammograms for a solution containing  $2.5$  mg of PTMA, **3**, in  $10$  mL of  $0.1$  mol  $L^{-1}$   $Bu_4NPF_6/CH_3CN$ . WE, GC ( $0.07$  cm $^2$ );  $\nu = 100$  mV  $s^{-1}$ . Different inversion potential conditions are depicted. All voltammetric signals are indicated.

transfer ( $E^0 = 0.37$  V vs  $Fc^+/Fc$ ,  $\Delta E_p = 15$  mV). Also, a second irreversible oxidation signal, peak IIa, occurs at more positive potential values ( $E_{pIIa} = 1.6$  V vs  $Fc^+/Fc$ ). It should be noticed that the presence of peak IIa has not been presented during previous studies with this polymer.<sup>5–12</sup> This is probably because the previous studies have been performed in solvents with a potential window shorter than that of acetonitrile.

It is noticeable that the voltammograms of both PTMA (Figure 11) and compound **2** (Figure 9B) show a similar value of current intensity for peaks Ia. This similarity can be rationalized by considering that, at a constant scan rate, the current peak is proportional to the concentration of electroactive species, the diffusion coefficient and the electron number. In both experiments, the solutions were prepared with a similar amount of these compounds:  $2.4$  and  $2$  mg, respectively. However, considering that the molecular weight of compound **2** is too low ( $240$  g  $mol^{-1}$ ) with respect to the polymer ( $36240$  g  $mol^{-1}$ ), the molar concentration of PTMA as well as

its diffusion coefficient must be the lowest. This result indicates that the only factor that contributes to increase the current intensity for PTMA until  $30$   $\mu A$  is the electron number, which must be close to  $151$  ( $36240/240$ ). This value corresponds to the number of methacryloyloxy-TEMPO units present in the polymer structure, which are oxidized at the level of peak Ia shown in Figure 11.

PTMA shows paramagnetic activity ( $g \approx 2$ ), characterized by the presence of a broad central signal (Linewidth around  $10$  G). This signal did not improve its resolution by adjusting both the power of irradiated microwaves or modulation amplitude (dashed line, Figure 12). Because of the significant broadness of

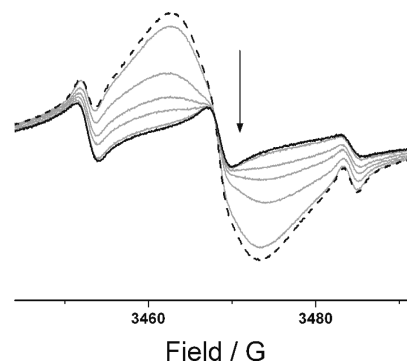


**Figure 12.** Spectroelectrochemical-ESR spectra of a solution containing  $2.5$  mg of PTMA, **3**, in  $4$  mL of  $0.1$  mol  $L^{-1}$   $Bu_4NPF_6/CH_3CN$ . WE, Pt ( $0.7$  cm $^2$ ). Applied potential,  $0.6$  V vs  $Fc^+/Fc$ . Dashed line indicates initial spectrum. Solid line indicates spectrum obtained after  $50$  min of electrolysis. Arrow indicates variations of the spectra upon increasing electrolysis times.

the central signal, it can be presumed that the amount of radical species related to the central signal is high as the ESR signals would show coalescence due to fast spin exchange mechanisms.<sup>39</sup> This spectral pattern, obtained in solution, is similar to that reported in a previous study where solid composite electrodes were prepared with PTMA,<sup>10</sup> suggesting that spin density distribution is not affected by the medium in which the polymer is analyzed. It has also been reported that this broadening is related to interchain interaction within the polymer structure, which support the proposed fast spin exchange process suggested.

Spectroelectrochemical-ESR measurements applying potential values more positive than peak Ia lead to the disappearance of the central signal (Figure 12). In this process, another spectral structure becomes visible, showing a triplet hyperfine coupling structure (HFCC =  $15.86$  G,  $g = 2.0104$ , solid line, Figure 12). This result indicates that the original spectrum (dashed line, Figure 12) is the sum of two overlapping spectra arising from two different organic radical species. Upon applying potential values more positive than peak IIa ( $1.7$  V vs  $Fc^+/Fc$ ), the second radical structure is consumed (Figure 13). This behavior, along with the spectral structure for this signal, is analogous to that reported for nitroxide radicals proceeding from TEMPO species, considering only the first signal (peak Ia, Figure 11).<sup>10</sup> However, the corresponding voltammetric signal is not reversible for the case of PTMA (peak IIa, Figure 11), indicating that the corresponding formation of the cationic species is followed by a coupled chemical process, probably with the nucleophilic solvent, such as in the case of the Ritter reaction in which carbocations react with acetonitrile.<sup>40</sup>

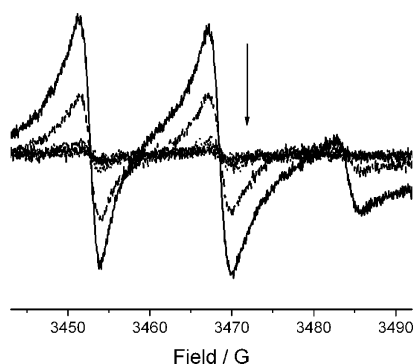
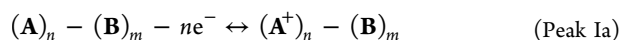


**Figure 13.** Spectroelectrochemical-ESR spectra of a solution containing 2.5 mg of PTMA, **3**, in 4 mL of 0.1 mol L<sup>-1</sup> Bu<sub>4</sub>NPF<sub>6</sub>/CH<sub>3</sub>CN after being electrolyzed for 50 min at 0.6 V vs Fc<sup>+</sup>/Fc. WE, Pt (0.7 cm<sup>2</sup>); applied potential, 1.7 V vs Fc<sup>+</sup>/Fc. Dashed line, initial spectrum; solid line, spectrum obtained after 50 min of electrolysis. Arrow indicates variations of the spectra upon increasing electrolysis times.

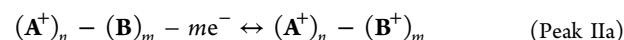
To determine the amount of spins related to each particular radical, double integration of the experimental spectra obtained both before performing electrochemical oxidation of the sample and later by oxidizing the first radical species (dashed and solid lines, Figure 12) was performed.<sup>38</sup> With this procedure, a total of  $5.29 \times 10^{18}$  spins was determined for the sum of both radical species present in PTMA (2 mg of the polymer). Considering the molecular weight of PTMA, this spin count is close to the value expected considering a mean proportion of 151 repetitive units in the structure of the polymer ( $\sim 5.18 \times 10^{18}$  spins). Therefore, the total number of spins detected by ESR indicates that the radical content in the polymer structure is about 100% of the expected value. This calculation was validated by evaluating the variations of the molar magnetic susceptibility of PTMA at temperatures above 81 K (Inset, Figure 4), where a fraction of 94% of spin character was determined per repetitive unit.<sup>34</sup> However, only 22% of these spins ( $\sim 1.17 \times 10^{18}$  spins) were related to nitroxide radicals, oxidized at peak IIa, while the remaining 78% of radical species have a different spin density, oxidized at peak Ia (Figure 11).

The large shift in potential values ( $E_{\text{pIa}} - E_{\text{pIIa}} \approx 1.25$  V) for the oxidation of both types of nitroxide radicals in the polymer structure can be associated to changes in the electronic charge occurring for the chain being oxidized, due to the high amount of electrons being removed at peak Ia (about  $118 e^-$ );<sup>38</sup> this significant decrease in electron density leads to the formation of a structure that becomes less prone to be oxidized, requiring more positive potential values to do so (Figure 11, peak IIa). This effect could be related to the highly positive structure acting as a strong electron-withdrawing group,<sup>36,37</sup> resulting in the large shift in potential values. Peak IIa has not been addressed in previous studies concerning PTMA, probably due to the less positive value of the anodic barrier occurring for the solvents employed in such works (e.g., propylene carbonate).<sup>5-10</sup> By representing the polymer oxidizable sites as **A** (isotactic) and **B** (hetero/syndiotactic domains), respectively, the electrochemical processes occurring can be represented schematically as follows

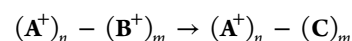


This reaction is electrochemically reversible, as denoted by the presence of peak Ic (Figure 11). The product of this reaction carries an  $n$  positive charge, which would be approximately +118

for each polymer chain being oxidized, thus rendering sites marked **B** as more difficult to be oxidized. **B**-labeled sites would then be oxidized at the second peak following the reaction



These **B**<sup>+</sup> species undergo a coupled chemical reaction to generate non-electrochemically active species **C**



Sites **A**<sup>+</sup> are not affected in this chemical process as peak Ic still appears during the inverse scan (Figure 11). This suggests that, even though the charging of the polymer determines the potential values at which the secondary radical is being oxidized, it does not determine specific reactions on each site. It should be noticed that, within the polymer structure, an irregular distribution of the sites is expected, but in the overall, the proportions are consistent with the experimental tacticity. Because of the charging of the chain occurring at both peaks, it is possible that specific solvation of the cationic species can determine the potential values of these signals, an issue that is currently under study.

As these two radical species are present in the structure of PTMA, their properties and relative proportions could be related to the microstructure present in the entire chain.<sup>20</sup> It would be reasonable to correlate this variety of configurations to different chemical environments for nitroxide radicals within iso-, hetero-, and syndiotactic triads. In fact, the finding that 78% of radical species (peak Ia, Figure 11) within PTMA behaving in a very different way than the remaining 22% (peak IIa, Figure 11), from spectroelectrochemical studies, and the quantification of 84% of isotactic triads and 16% of heterotactic/syndiotactic triads (determined by signal deconvolution of high temperature <sup>1</sup>H NMR spectra, Figures 7 and 8) strongly suggests, within experimental error, a correlation between spectroelectrochemical behavior and microstructural features. The reversible behavior of peak Ia (Figure 11) would be related to the oxidation of a high number of structurally similar radicals in the isotactic microstructure, leading to a broad spectral line width (Figure 12).<sup>39</sup> This broadening can also be originated from interchain effects by interaction of radical species within PTMA structures, as has been reported in independent studies.<sup>10</sup> However, the species being oxidized at peak IIa, corresponds to radical species in the syndiotactic/heterotactic domain of the polymer. It should be noticed that the hyperfine structure of the involved radicals (Figure 13) resembles more so those from the original TEMPO structures (Figure 10), probably due to less pronounced dynamic spin exchange processes<sup>39</sup> as the radical sites are spatially more separated than those considering isotactic domains. The presence of both types of radical species has not been considered in earlier reports, presumably due to the lack of characterization on extended oxidation potential scales, due to the solvents employed.<sup>5-12</sup>

In an isotactic triad, the central monomeric unit is flanked by two monomers with the same configuration; in comparison, heterotactic triads present the central unit as a monomer with the same configuration at one side and a monomer with the opposite configuration at the other side, while, in a syndiotactic triad, the central monomer is surrounded by two units with opposite configuration. This would make reasonable to consider that this variety of configurations would lead to different chemical environments for nitroxide radicals within iso-, hetero-, and syndiotactic triads.

## CONCLUSIONS

In this work, spectroscopic, thermal, and electrochemical characterization results are presented for the redox active polymer poly(4-methacryloyloxy-tetramethylpiperidine-*N*-oxyl), PTMA, synthesized by group transfer polymerization (GTP) and its precursors 4-hydroxy-tetramethylpiperidine-*N*-oxyl (HO-TEMPO) and 4-methacryloyloxy-tetramethylpiperidine-*N*-oxyl (MO-TEMPO). The procedure presented in this work is helpful to determine the content of redox useful units in a TEMPO based polymer like PTMA. As a whole, the facts exposed above validate the assertion that PTMA synthesized by GTP (known for yielding polymer with 100% of the expected radical species),<sup>14</sup> at the experimental conditions used in this work, is a polymer with 84% of isotactic triads, 12% of heterotactic triads, and 4% of syndiotactic triads (the combined percentages of hetero- and syndiotactic triads is 16% of the total triads). In fact, the finding of 78% of radical species within PTMA behave in a very different way that the remaining 22% after spectroelectrochemical studies and the quantification, by high temperature <sup>1</sup>H NMR, of 84% of isotactic triads and 16% of heterotactic/syndiotactic triads strongly suggests, within experimental error, a correlation between spectroelectrochemical behavior and microstructural features. The above presented information is important in battery applications since only N–O radicals oxidized reversibly at peaks Ia/Ic (Figure 11) are considered to react under the operation conditions of a battery or capacitor. However, other types of radical species that are energetically inaccessible during the oxidation of the polymer, can determine the efficiency of the final battery. Therefore, it is important to have not only a large number of radical redox units attached to the polymer by a route of polymerization (GTP) but also a large number of these groups being oxidized during low energetic conditions carrying out the reversible redox process. In this way, and compared with PTMA obtained using radical polymerizations,<sup>5–12</sup> the induction of tacticity is a critical parameter in the development of materials more efficient as it has been found that, even using PTMA carrying 100% of radical concentration in the polymer, the battery behavior is only active in ca. 80% of the polymer.<sup>14</sup>

## ASSOCIATED CONTENT

### Supporting Information

<sup>1</sup>H and <sup>13</sup>C NMR spectra of the precursors and PTMA, along with proposed mass spectra fragmentation pathways for compound 1 and 2. Deconvolution procedures are also included. This material is available free of charge via the Internet at <http://pubs.acs.org>.

## AUTHOR INFORMATION

### Corresponding Author

\*(C.F.) Tel: (52) 442 2116000, ext. 7849. Fax: (52) 442 211 6001. E-mail: [ultrabuh@yahoo.com.mx](mailto:ultrabuh@yahoo.com.mx) or [cfrontana@cideteq.mx](mailto:cfrontana@cideteq.mx). (J.C.) Tel: (52) 555 804 4625. E-mail: [jcam@xanum.uam.mx](mailto:jcam@xanum.uam.mx).

### Present Address

<sup>||</sup>Centro de Investigación y Desarrollo Tecnológico en Electroquímica, Parque Tecnológico Querétaro Sanfandila, 76703 Pedro Escobedo, Querétaro, México.

### Notes

The authors declare no competing financial interest.

## ACKNOWLEDGMENTS

We acknowledge Mrs. Isabel Chávez, Rocío Patiño, Javier Pérez, Elizabeth Huerta, Ma de los Angeles Peña, M. Nieves Zavala, and Atilano Gutierrez for their technical assistance and to Dr. Angel Romo-Urbe (Instituto de Ciencias Físicas -UNAM) for the DMA analysis. Also, we acknowledge the assistance of Professor Roberto Escudero (IIM-UNAM) for his help on obtaining magnetic susceptibility measurements. Financial supports from the CONACyT-Mexico projects No. 57856, No. 60686, and No. 107037, PAPIIT-UNAM 202011, and Instituto de Ciencia y Tecnología del DF project PICCO11-22 are also acknowledged. L.H. and C.F. thank CONACyT-Mexico for financial support for their Ph.D. and postdoctoral studies, respectively. H.A.L.-P. thanks SNI Mexico for financial support for his B. in Sc. studies.

## REFERENCES

- (1) Zhou, H. S.; Li, D. L.; Hibino, M.; Honma, J. *Angew. Chem.* **2005**, *117*, 807.
- (2) Aric, M. A. S.; Bruce, P. G.; Scrosati, B.; Tarascon, J. M.; van Schalkwijk, W. *Nat. Mater.* **2005**, *4*, 366.
- (3) Huang, L.; Yang, Y.; Xue, L. J.; Wei, H. B.; Ke, F. S.; Li, J. T.; Sun, S. G. *Electrochem. Commun.* **2009**, *11*, 6.
- (4) Wachtler, M.; Winter, M.; Besenhard, J. O. *J. Power Sources* **2002**, *105*, 151.
- (5) Nakahara, K.; Iriyama, J.; Iwasa, S.; Suguro, M.; Satoh, M.; Cairns, E. J. *J. Power Sources* **2007**, *163*, 1110.
- (6) Qu, J.; Khan, F. Z.; Satoh, M.; Wada, J.; Hayashi, H.; Mizoguchi, K.; Masuda, T. *Polymer* **2008**, *49*, 1490.
- (7) Nakahara, K.; Iwasa, S.; Satoh, M.; Morioka, Y.; Iriyama, J.; Suguro, M.; Hasegawa, E. *Chem. Phys. Lett.* **2002**, *359*, 351.
- (8) Kim, J.-K.; Cheruvally, G.; Choi, J. W.; Ahn, J. H.; Choi, D. S.; Song, C. E. *J. Electrochem. Soc.* **2007**, *154*, A839.
- (9) Nakahara, K.; Iriyama, J.; Iwasa, S.; Suguro, M.; Satoh, M.; Cairns, E. J. *J. Power Sources* **2007**, *165*, 870.
- (10) Nishide, H.; Iwasa, S.; Pu, Y. J.; Suga, T.; Nakahara, K.; Satoh, M. *Electrochim. Acta* **2004**, *50*, 827.
- (11) Kim, J. K.; Cheruvally, G.; Ahn, J. H.; Seo, Y. G.; Choi, D. S.; Lee, S. H.; Song, C. E. *J. Ind. Eng. Chem.* **2008**, *14*, 371.
- (12) Nishide, H.; Suga, T. *Electrochem. Soc. Interface* **2005**, 32.
- (13) Li, H.-Q.; Zou, Y.; Xia, Y.-Y. *Electrochim. Acta* **2007**, *52*, 2153.
- (14) Bugnon, L.; Morton, C. J. H.; Novak, P.; Vetter, J.; Nesvadba, P. *Chem. Mater.* **2007**, *19*, 2910.
- (15) Brière, R.; Lemaire, H.; Rassat, A. *Bull. Soc. Chim. Fr.* **1965**, 3273.
- (16) Allgaier, J.; Finkelmann, H. *Makromol. Chem. Rapid Commun.* **1993**, *14*, 267.
- (17) Morales-Morales, J. A.; Frontana, C.; Aguilar-Martínez, M.; Bautista-Martínez, J.; Gonzalez, F. J.; Gonzalez, I. *J. Phys. Chem. A* **2007**, *111*, 8993.
- (18) Savéant, J. M. *Elements of Molecular and Biomolecular Electrochemistry: An Electrochemical Approach to Electron Transfer Chemistry*; Wiley Interscience: New York, 2006.
- (19) Gritzner, G.; Küta, J. *Pure Appl. Chem.* **1984**, *4*, 461.
- (20) Akita, T.; Mazakati, Y.; Kobayashi, K. *Mol. Cryst. Liq. Cryst.* **1997**, *306*, 257.
- (21) Cervantes-Uc, J. M.; Cauich-Rodríguez, J. V.; Vázquez-Torres, H.; Licea-Claverie, A. *Polym. Degrad. Stab.* **2006**, *91*, 3312.
- (22) Peyser, P. Glass Transition Temperature of Polymers. In *Polymer Handbook*, 3rd ed.; Brandup, J., Immergut, E. H., Eds.; Wiley: New York, 1989; Chapter VII, pp 210–212.
- (23) Kim, J.-K.; Cheruvally, G.; Choi, J.-W.; Ahn, J.-H.; Lee, S. H.; Choi, D. S.; Eui Song, C. *Solid State Ionics* **2007**, *178*, 1546.
- (24) Ferry, J. D. *Viscoelastic Properties of Polymers*, 3rd ed.; John Wiley & Sons, Inc.: New York, 1980; pp 448–451.
- (25) Otsuka, T.; Okuno, T.; Awaga, K.; Inabe, T. *J. Mater. Chem.* **1998**, *8*, 1157.

- (26) Akita, T.; Mazakati, Y.; Kobayashi, K. *J. Chem. Soc. Chem. Commun.* **1995**, 1861.
- (27) Pontillon, Y.; Akita, T.; Grand, A.; Kobayashi, K.; Lelievre-Berna, E.; Pécaut, J.; Ressouche, E.; Schweitzer, J. *J. Am. Chem. Soc.* **1999**, *121*, 126.
- (28) Mulay, L. N.; Mulay, I. L. Static Magnetic Techniques and Applications. In *Physical Methods of Chemistry, Determination of Chemical Composition and Molecular Structure*; Hamilton, M. D., Rossiter, B. W., Eds.; John Wiley & Sons: New York, 1987; Vol. 3, Chapter 3.
- (29) Maspoch, D.; Catala, L.; Gerbier, P.; Ruiz-Molina, D.; Vidal-Gancedo, J.; Wurst, K.; Rovira, C.; Veciana, J. *Chem.—Eur. J.* **2002**, *8*, 3635.
- (30) Maspoch, D.; Catala, L.; Gerbier, P.; Ruiz-Molina, D.; Vidal-Gancedo, J.; Wurst, K.; Rovira, C.; Veciana, J. *Chem.—Eur. J.* **2002**, *8*, 3635.
- (31) Webster, O. W. Group Transfer Polymerization: Mechanism and Comparison with Other Methods for Controlled Polymerization of Acrylic Monomers. In *New Synthetic Methods (Advances in Polymer Science)*; Springer: Berlin, Germany, 2004; Vol. 167.
- (32) Frisch, H. L.; Mallows, C. L.; Bovey, F. A. *J. Chem. Phys.* **1966**, *45*, 1565.
- (33) Bovey, F. A. *Pure Appl. Chem.* **1967**, *15*, 349.
- (34) Shapiro, Y. E. *Bull. Magn. Reson.* **1985**, *7*, 27.
- (35) Bovey, F. A.; Mirau, P. A. *NMR of Polymers*; Academic Press: New York, 1996.
- (36) Hansch, C.; Leo, A.; Taft, R. W. *Chem. Rev.* **1991**, *91*, 185.
- (37) Zuman, P. *Substituent Effects in Organic Polarography*; Plenum Press: New York, 1967.
- (38) López-Peña, H. A.; Hernández-Muñoz, L. S.; Cardoso, J.; González, F. J.; González, I.; Frontana, C. *Electrochem. Commun.* **2009**, *11*, 1369.
- (39) Weil, J. A.; Bolton, J. R. *Electron Paramagnetic Resonance: Elementary Theory and Practical Applications*; Wiley-Interscience: New York, 2007.
- (40) Smith, M. B.; March, J. *March's Advanced Organic Chemistry*, 6th ed.; John Wiley & Sons: New York, 2007; p 1458.